



Low-level laser therapy as a modifier of erythrocytes morphokinetic parameters in hyperadrenalinemia

Anna V. Deryugina¹ · Marina N. Ivashchenko² · Pavel S. Ignatiev³ · Irina V. Balalaeva⁴ · Alexander G. Samodelkin²

Received: 4 December 2018 / Accepted: 15 February 2019 / Published online: 4 March 2019
© Springer-Verlag London Ltd., part of Springer Nature 2019

Abstract

Low-level laser therapy (LLLT) is widely used in clinical practice for treatment of various pathologies. It is assumed that LLLT impact on microcirculation is among the mechanisms underlying its therapeutic effect. The microcirculation disorder is observed in the pathogenesis of any inflammatory process and is significantly influenced by red blood cells (RBCs). On this point, studying the RBCs morphology under the influence of LLLT on altered organism is of scientific interest and practical importance. The aim of the present study was to analyze the LLLT effect on morphokinetic parameters of RBCs in hyperadrenalinemia. The LLLT effect was analyzed on rats intraperitoneally injected with adrenaline hydrochloride solution (0.1 mg/kg). As the comparison groups, the effects of LLLT, adrenaline, or saline injection as well as the parameters of intact animals were studied. LLLT was applied on the occipital region of rats for 10 min. The light irradiation with pulse frequency 415 Hz at 890 nm wavelength and average power density in the plane of the output window at $193 \mu\text{W}/\text{cm}^2$ was used. The dynamics of morphological characteristics of RBCs was studied by phase interference microscopy; the RBC electrophoretic mobility was tested by microelectrophoresis technique; photometric analyses of the RBCs amount, hemoglobin content, and osmotic fragility were performed. The adrenaline injection resulted in a significant increase in the amount of RBC pathological forms and a decrease in discocytes and normocytes by more than 50%. An increase in the optical density of RBC phase portraits, a decline in osmotic resistance, and electronegativity of RBC membranes and a reduction of their number in peripheral blood were also registered. The revealed effects persisted for 1 week after the adrenaline administration. LLLT did not significantly impact on the RBC parameters 1 h after adrenaline injection. However, a day later, LLLT reduced the severity of the adrenaline effect on RBSs, which was manifested in a decreased amount of the pathological forms of RBCs, restored RBC phase portraits, higher electrophoretic mobility and osmotic resistance, and RBSs amount in peripheral blood restored up to the level of intact animals. We suppose that the mechanism of LLLT action is realized both at cellular level through the laser radiation effect on RBC membranes, and at systemic level through the activation of stress-realizing systems of the organism with subsequent limitation of inflammatory response.

Keywords Low-level laser therapy (LLLT) · Phase interference microscopy · Red blood cells · Hyperadrenalinemia

✉ Anna V. Deryugina
derugina69@yandex.ru

¹ Department of Physiology and Anatomy, Institute of Biology and Biomedicine, Lobachevsky University, 23 Gagarin Ave., Nizhny Novgorod 603950, Russia

² Department of Physiology and Biochemistry of Animals, Nizhny Novgorod State Agricultural Academy, 97 Gagarin Ave., Nizhny Novgorod 603107, Russia

³ Yalamov Urals Optical-Mechanical Plant, 33B Vostochnaya Str., Yekaterinburg 620100, Russia

⁴ Department of Biophysics, Institute of Biology and Biomedicine, Lobachevsky University, 23 Gagarin Ave., Nizhny Novgorod 603950, Russia

Introduction

The effectiveness of low-level laser therapy (LLLT) has been demonstrated in numerous experimental and clinical studies for correction of functional disorders, suppression pain, and anti-inflammatory reactions in patients with cardiological, neurological, endocrinological, and oncological diseases [1, 2]. However, there is still no generally accepted concept about mechanisms of LLLT action on biological objects. It was shown that some clinical and photobiological effects of LLLT may be manifested more or less intensively and depend on various factors such as wavelength, power, and type of irradiation. Moreover, the overall influence on cells, particular

tissue, and whole organism may be either positive or negative [3]. It cannot be ruled out that laser irradiation may provoke a considerable inhomogeneity of a temperature gradient in tissues [4].

The direct effect of LLLT on biochemical processes is mediated by photoacceptors. LLLT induces biochemical changes in cells due to the absorption of photons by cellular photoreceptors [5]. The enzyme cytochrome c-oxidase is considered as an endogenous photoacceptor [6], leading to the induction of ATP synthesis [7, 8]. The important role is played by LLLT-induced generation of reactive oxygen species (ROS). The mediating effect of ROS is associated with the modulation of nitric oxide synthase (iNOS) [9] and protein kinase C activity [10], expression of specific genes associated with a control of proliferation [11]. An activation of redox-dependent signaling affects expression of a number of transcription factors [12] and pro-inflammatory cytokines [13, 14], and increases the activity of heat shock proteins [15].

The revealed variety of cell responses to the action of LLLT is reflected in the final complex response of organs and systems of the organism. It should be noted that a pathological process develops on the background of disadaptation of the organism, which is often based on sympathetic hyperactivity. For example, pain syndrome, trauma, and hemodynamic disorder are accompanied by transient hyperadrenalinemia. Activation of sympathoadrenal system exacerbates the progress of ischemic heart disease. Hyperadrenalinemia can accompany the development of tumors, recurrent myocardial infarction, and sudden death [16, 17].

A damaging factor provokes the development of the inflammatory process [18], which passes in its development through a phase change in the ischemia-reperfusion cycle with impaired microcirculation. Any influence reducing the prolonged ischemic stage will have a beneficial effect on the subsequent development of the disease. It has been reported that laser irradiation can increase a linear blood flow velocity and vascular diameter [19]. The significant role of RBCs in microcirculation must be mentioned. In turn, RBCs are sensitive to the action of adrenaline, which affects their membrane fluidity and deformability [20]. Thus, issues related to the LLLT effect on the morphological parameters of RBCs are of current interest.

The aim of the present work was to study the LLLT effect on the morphological parameters of rat RBCs in hyperadrenalinemia conditions.

Materials and methods

Animals and anesthesia conditions

The study was conducted on 50 non-linear white female rats aged 3.5–4 months weighing 200 ± 20 g. The animals were

housed and the experiment was performed in accordance with Universal Declaration of animal rights and with the Order of the Ministry of Health of the Russian Federation No. 199n of April 1, 2016, “Approval of the good laboratory practice.”

All the operative treatments were accompanied by the use of zoletil and xylazine anesthesia in the following combination: zoletil (Virbac, France) 0.3 mg intramuscularly; xylazine (Nita-Farm, Russia) 0.8 mg intramuscularly; and 0.1% atropine sulfate in 0.01 ml subcutaneously. The dosages were calculated to 100 g of animal weight. The effect of anesthesia was verified by disappearance of the reaction to pain stimuli (paw prick) and inhibition of the corneal reflex.

Treatment groups

Animals were randomly assigned into four treatment groups (10 rats per group) with the following treatment schemes. The animals of group 1 (“adrenaline” group) received a single intraperitoneal injection of adrenaline hydrochloride solution (0.1 mg/kg). The animals of group 2 (“adrenaline+LLLT” group) received an adrenaline hydrochloride injection (0.1 mg/kg) and in 30 min were exposed to laser irradiation for LLLT. The animals of group 3 (“LLLT” group) were treated with LLLT. The group 4 (“intact” group) comprised control intact animals. The animals of group 5 (“saline” group) received a saline solution injection.

LLLT procedure

The time point for LLLT was chosen based on adrenaline pharmacodynamics: The maximum effect is observed 20 min after subcutaneous injection; the rate of reaction development after intraperitoneal administration is variable. The preliminary determination of the adrenaline concentration in blood of the rats by ELISA method showed its maximum increase by 30 min after administration.

For LLLT, the rats placed in an open chamber were exposed to laser irradiation at the occipital region for 10 min from a distance of 5 mm. The duration of the exposition was determined according to the time for a standard physiological procedure. The therapeutic laser apparatus “Uspekhn” (Voskhod, Russia) was used as an irradiation source. The pulsed irradiation with wavelength at 890 nm, pulse frequency at 415 Hz, and average power density in the plane of the output window at $193 \mu\text{W}/\text{cm}^2$ was applied.

Blood sampling in adrenaline, adrenaline+LLLT, and control groups was performed from the sublingual vein 1 h, 1 day, and 1 week after adrenaline administration. In LLLT group, the blood was sampled 30 min after the beginning of the experiment to ensure time compatibility between adrenaline+LLLT and LLLT groups.

Study of RBCs morphology

The RBC amount and hemoglobin concentration were analyzed using an automatic hematology analyzer Abacus Junior Vet (Diatron, Austria).

The RBC morphology was studied in unwashed samples, since the previous experiments had shown a positive effect of the presence of blood plasma components on the preservation of the cell form. The drop of the cell suspension was placed on the microscope slide between two plastic cover glasses. Vaseline oil was applied to seal the perimeter and prevent liquid flows and drying of the spacemen. RBCs were shown to preserve the normal discoid form in such the microchamber during several hours and up to a day.

The cell morphology was studied using laser interference microscope MIM-340 (Yekaterinburg, Russia) equipped with an objective lens $\times 30$ (NA = 0.65). Two modes of image acquisition were applied: the phase contrast mode, sensitive to the object thickness, and the backscattering mode, sensitive to the displacement of the object boundaries. The object was scanned by a laser with 650-nm wavelength. Images were captured with CCD camera VS-415U (NPK Videoscanner, Russia) with resolution 782×582 pixels. The frame size was $195 \times 145 \mu\text{m}$. The lateral resolution of the method is up to 15 nm, the axial resolution is 0.1 nm, and the relief depth is up to 600 nm. The time for an image acquisition was about 10 s. The signal during the generation of the phase portrait was normalized by the wavelength. The reconstruction of the phase images was carried out using the phase step method (WinPhast software, USA); further image processing was performed with FIJI and Microcal Origin Software (Microcal Inc., USA) [21].

RBC morphometry was performed by integral analysis of the cell population (100 cells in each treatment group) by morphological characteristics: the percentage of cell distribution in shape and diameter.

Analysis of RBCs electrophoretic mobility

The RBCs were washed thrice with 0.85% sodium chloride solution, being collected each time by centrifuging at 1500 rpm for 10 min (PE-6910, Ekros, Russia). The blood was stabilized with heparin (5 U/ml). The erythrocytes electrophoretic mobility (EEM) was tested by microelectrophoresis technique [22]. The RBC suspension (20 μl) was diluted with 10 mM Tris-HCl buffer (pH 7.4) and placed in an electrophoresis chamber. The time for RBCs passing 100 μm distance at 8 mA current was recorded.

The EEM value was defined using the equation:

$$U = S/T \times H,$$

where S is the distance passed by the cells, T is the time, and H is the gradient of electric potential.

The gradient of electric potential H was determined from the equation:

$$H = I/g\chi,$$

where I is the amperage, g is the chamber cross section, and χ is the electrical conductivity of the media.

Measuring of RBCs osmotic fragility

The osmotic fragility (OF) of RBCs was measured using a series of sodium chloride solutions with concentrations from 0.9 to 0.1% with 0.1% step. The suspension of washed RBCs (20 μl) was added to 0.5 ml of the sodium chloride solution. After 30 min incubation, RBCs were removed by centrifugation. The degree of hemolysis was determined photometrically by measuring hemoglobin concentration in the supernatant at 540 nm using KFK 3-01 (Zagorsk Optical-Mechanical Plant, Russia) [23].

Statistical analysis

Statistical analysis was performed using ANOVA (BIOSTAT software). A value of $p < 0.05$ was considered as statistically significant.

Results

The analysis of interferograms of RBC of intact animals showed that 86% of the cells were represented by discocytes, 11% by echinocytes, and 2.5% by stomatocytes, and degeneratively altered cells were not detected (Fig. 1). Normocytes with a cell diameter of 7.0 to 7.7 μm prevailed and accounted for 85% of all RBCs (Fig. 2). Phase portraits of RBCs were represented by typical discocytes with a biconcave cell shape and a uniform distribution of hemoglobin: The wavelength of phase portraits was in the region of 500–600 nm (Fig. 3).

After LLLT, the percentage of the RBC morphological forms did not differ from the intact animals (Fig. 1). The proportion of normocytes also remained the same (Fig. 2). However, the phase portraits of the cells 1 h after LLLT exposure were characterized by the appearance of a large number of convexes and bulges in both discocytes and echinocytes (Fig. 4A). The wavelength of the RBCs phase portraits increased up to the region of 600–700 nm. One day later, the cell surfaces became smoother (Fig. 4B), although the phase portraits wavelength remained in the 600–700 nm region, which was significantly higher compared to RBCs of the intact animals. The recovery of the RBC phase portraits to that of the intact group were registered 1 week after the LLLT treatment.

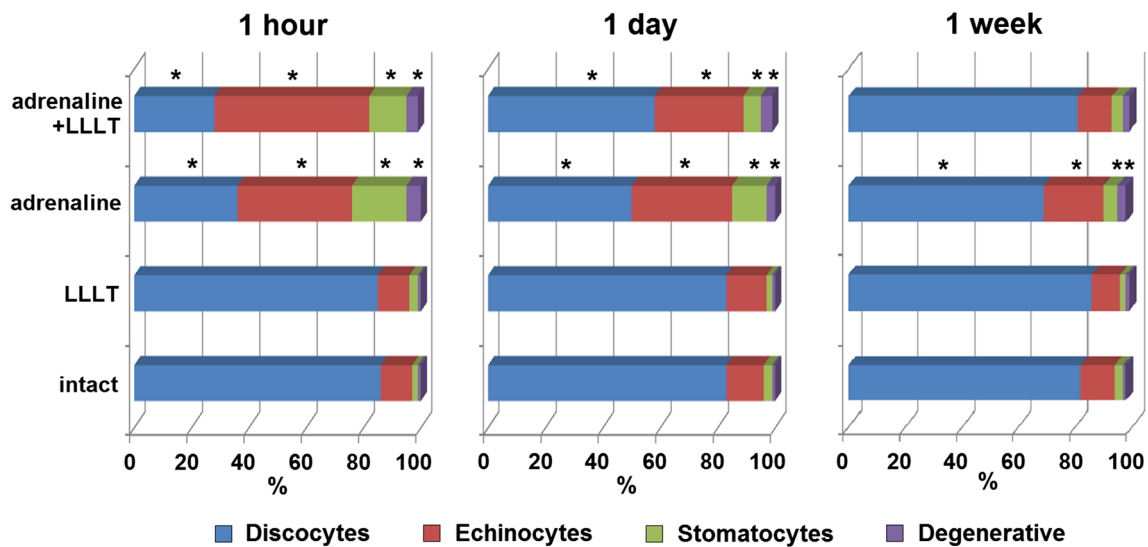


Fig. 1 Changes in RBC morphology induced by hyperadrenalinemia and LLLT an hour, a day, and a week after the treatment. The percentage of the RBC morphological forms is presented. Asterisk indicates values that differ from the value in the intact animals group at $p < 0.05$

The morphological heterogeneity of the RBCs pool was a characteristic feature under the action of adrenaline: A decrease in the number of discocytes with the corresponding increase in transitional (echinocytes, stomatocytes) and degenerative forms was significantly expressed at 1 h and 1 day after adrenaline administration (Fig. 1). Phase portraits of RBCs of the rats with hyperadrenalinemia at 1 h time point were characterized by the appearance of a large amount of echinocytes, an increased sphericity of the cells, and the appearance of degeneratively altered cells (Fig. 5A). In a day, the morphological modification of the RBCs was preserved: the diameter of the cells and the thickness in the edge region decreased, and the size of the central zone increased (Fig. 5B). One week after adrenaline administration, the discocytes had a reduced concave depth of the central zone

(Fig. 5C). Long wavelength in the 600–700 nm region prevailed in the RBC phase portraits. The RBC poikilocytosis was accompanied by anisocytosis. The normocyte amount decreased by 60% in 1 h on account of the rise in number of microcytes by 7 times and macrocytes by 1.5 times compared to the parameters of the intact group (Fig. 2). The recovery of the RBCs size to the normal values was not observed until the end of the experiment.

LLLT on the background of hyperadrenalinemia resulted in RBC characteristics similar to that after adrenaline administration at 1 h time point: An increase in the amount of the RBC modified forms with a decrease in discocytes (Fig. 1). In the adrenaline+LLLT group, the number of discocytes reduced by 67% due to an increase of echinocytes amount by five times, and stomatocytes by six times compared to the intact group.

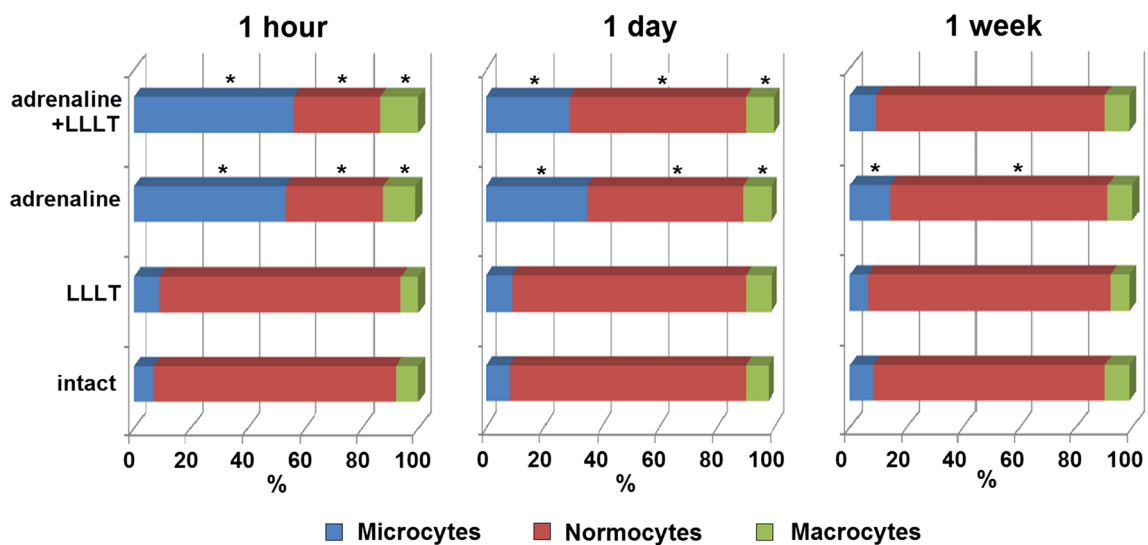


Fig. 2 Changes in RBCs size distribution induced by hyperadrenalinemia and LLLT an hour, a day, and a week after the treatment. The percentage of the RBC size groups is presented. Asterisk indicates values that differ from the value in the intact animals group at $p < 0.05$

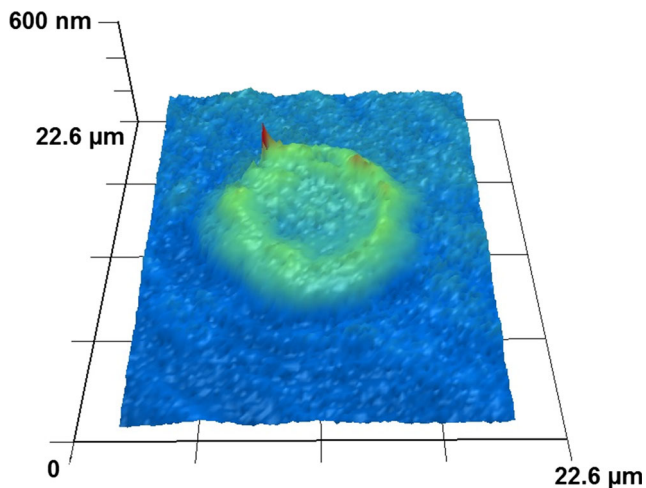


Fig. 3 3D phase portrait of a discocyte in the intact animals group.

Of note, the percentage of echinocytes in adrenaline+LLLT group was higher than in adrenaline group 1 h after treatment (Fig. 1). However, 1 day later, the dynamics of morphometric parameters in the studied groups changed, which was expressed in the prevalence of echinocytes and stomatocytes under the action of adrenaline compared to adrenaline+LLLT group. The total percentage of the pathologically changed RBCs remained elevated in both groups compared to the intact group. In a week, the morphological characteristics of RBCs were recovered under the action of LLLT on the

background of adrenaline to the values of the intact group. The phase portraits of RBCs revealed the growth of cell sphericity by 1 h after treatment (Fig. 6A) followed with a gradual decrease in sphericity and an increase in echinocytes percentage by 1 day (Fig. 6B). The RBC membrane had a heterogeneous phase height around the cell perimeter. LLLT on the background of adrenaline caused shortening of the wavelength in the RBC phase portraits to 600–650 nm by 1 day after treatment. By this time, an increase in the amount of normocytes by 13% and a decrease in the microcytes by 17% were registered compared with the adrenaline group. By 1 week, the percentage of RBCs size distribution recovered to normal values (Fig. 2).

Changes in the RBCs morphology were accompanied by changes in the RBC amount and hemoglobin concentration, as well as RBC electrokinetic parameters and osmotic fragility.

The adrenaline administration led to the reduced amount of RBCs and hemoglobin with the lowest values registered after 1 day of the observation (Table 1). LLLT caused a decrease of the RBC amount and hemoglobin at 1 h time point followed by recovery of the parameters by 1 day after treatment. LLLT was able to correct the adrenaline-induced reduction in the RBC amount and hemoglobin; in this case, the values of the parameters recovered during 1 week after treatment.

Adrenaline and LLLT were shown to have opposite effects on EEM. The adrenaline administration led to EEM decrease to 80–90% of the intact group values. On the contrary, LLLT

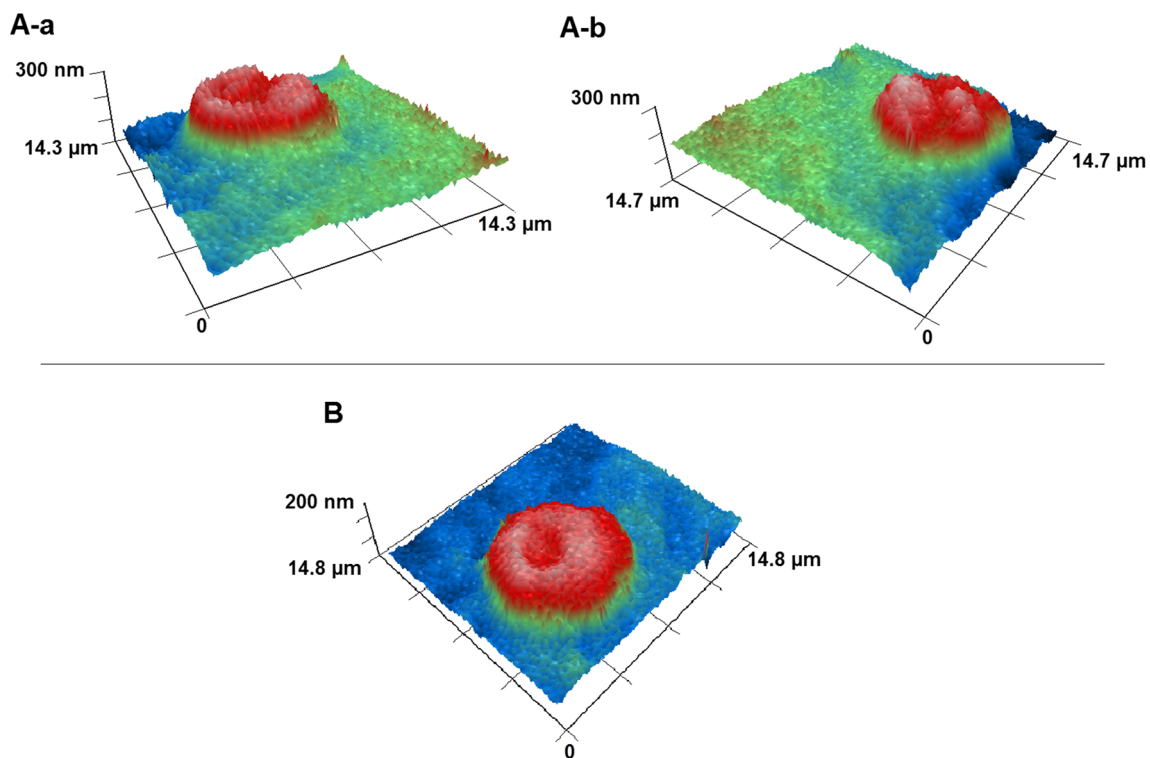


Fig. 4 3D phase portrait of RBCs in the “LLLT” animals group. **A** RBCs at 1 h after treatment; images of a discocyte (**A-a**) and an echinocyte (**A-b**) are presented. **B** A discocyte at 1 day after treatment.

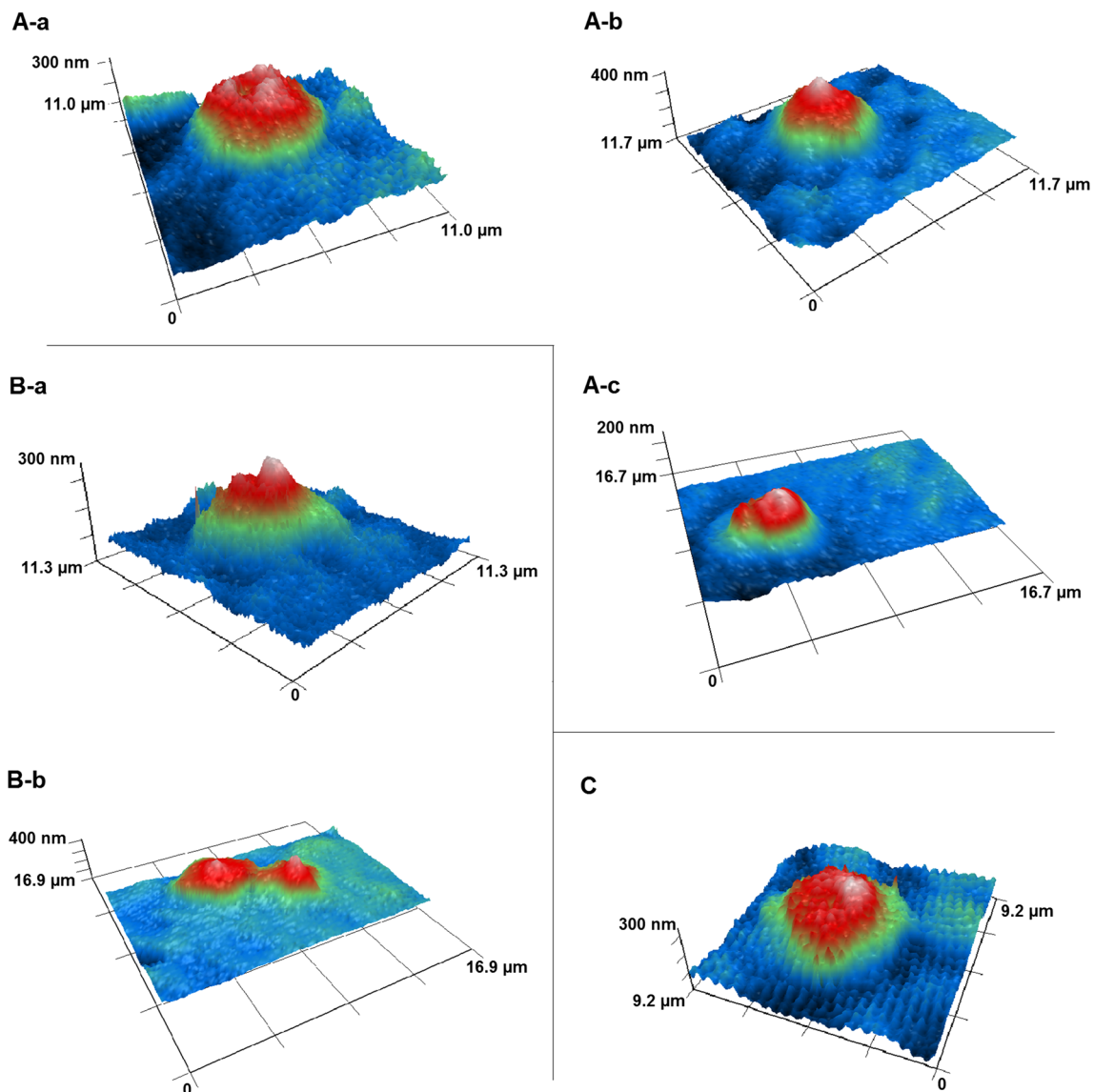


Fig. 5 3D phase portrait of RBCs in the “adrenaline” animals group. **A** RBCs at 1 h after treatment; images of an echinocyte (**A-a**), a spherocyte (**A-b**), and a degeneratively altered RBC (**A-c**) are presented. **B** RBCs at 1 day after treatment; images of an echinocyte (**B-a**), a spherocyte, and a degeneratively altered RBC (**B-b**) are presented. **C** A discocyte at 1 week after treatment.

induced EEM increase of 10–30%. In adrenaline+LLLT group, the initially reduced EEM value recovered during 1 day to the level of the intact animals (Table 1).

The osmotic fragility of RBCs was not affected by LLLT; no difference between intact and LLLT treated rats was registered (Fig. 7). On the contrary, the adrenaline administration caused a decline in the osmotic resistance observed throughout the course of the experiment. The significant change in the OF was observed already at 0.8% NaCl: The RBC resistance drops to 68% in 1 h and did not exceed 80% of the intact group values in a week.

LLLT was shown to abrogate the adrenaline effect on OF of erythrocytes to a large extent as early as 1 h after treatment. The reduced RBC resistance was registered at 0.7% NaCl (by 17% relative to the values of the intact group). One day later,

the negative effect was observed only at 0.5–0.6% NaCl (by 20 and 25%, respectively). After a week, the OF of the cells in adrenaline+LLLT group did not differ from that in the intact group. Of note, in adrenaline group, the RBC osmotic resistance was significantly reduced in the range of NaCl concentrations from 0.4 to 0.8%.

Discussion

The obtained results indicate the modifying potential of LLLT on the adrenaline-induced alterations in the morphological parameters of RBCs. Analysis of the RBCs morphology in adrenaline+LLLT group revealed a gradual recovery of the RBCs form starting 1 day after the alteration compared to

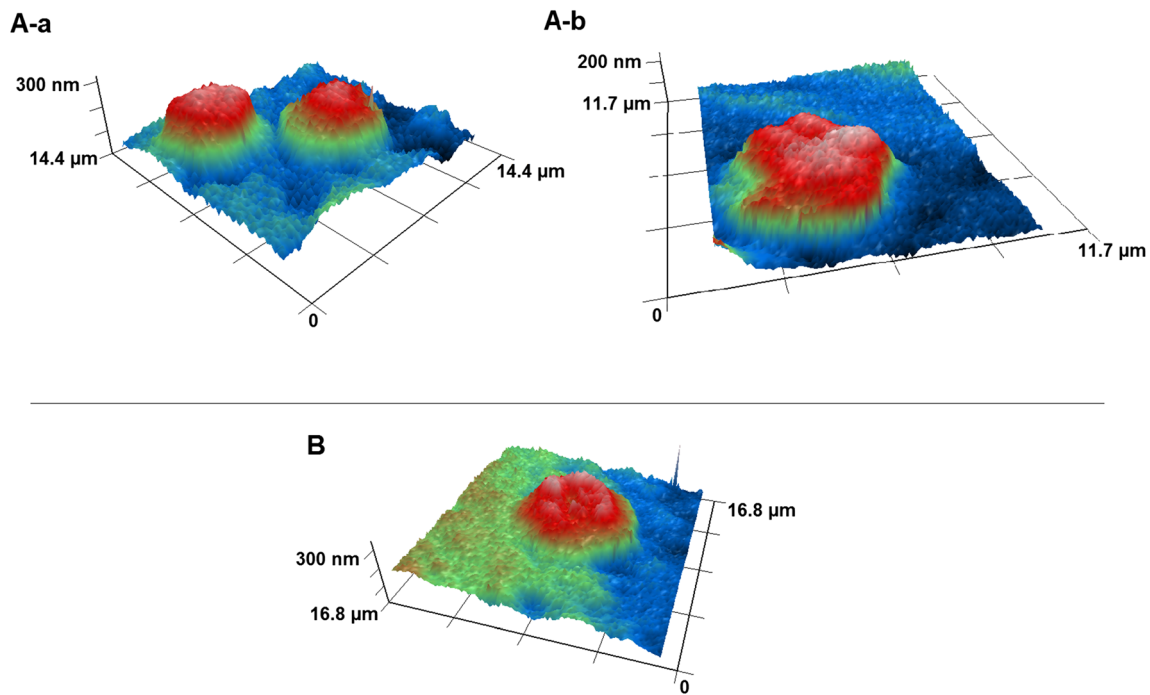


Fig. 6 3D phase portrait of RBCs in the “adrenaline+LLLT” animals group. **A** RBCs at 1 h after treatment; images of a spherocyte (**A-a**) and an echinocyte (**A-b**) are presented. **B** An echinocyte at 1 day after treatment.

adrenaline group, in which recovery of the parameters was not observed within 1 week. At the same time, it must be underlined that more pathologically changed RBC forms were detected in adrenaline+LLLT group 1 h after treatment as compared with adrenaline group, mostly due to the growth of a number of echinocytes and stomatocytes. The increase in the RBC pathological forms in both the groups at the initial stage of the study can be apparently explained by the development of a stress reaction. Discussing the results obtained, it should be noted that an enhancement of lipid peroxidation is commonly considered as a universal mechanism of cell damage under stressing conditions. Under LLLT, the light

absorption by porphyrins can cause the additional ROS generation [24], thus promoting the adrenaline-induced oxidative stress. The enhancement of lipid peroxidation initiates a cascade of events that manifests in a change in the morphological structure of the cells. The presumable sequence of events may be as follows: (i) Na,K-ATPase is a lipid-dependent enzyme whose activity decreases with the development of a stress reaction and is consistent with a lowered surface charge of RBCs; (ii) the inhibition of Na,K-ATPase activity leads to an increase in the intracellular concentration of Ca^{2+} due to an activation of $\text{Na}^+ / \text{Ca}^{2+}$ exchange mechanism [25]; (iii) the rise in intracellular Ca^{2+} activates Ca^{2+} -dependent K^+ -

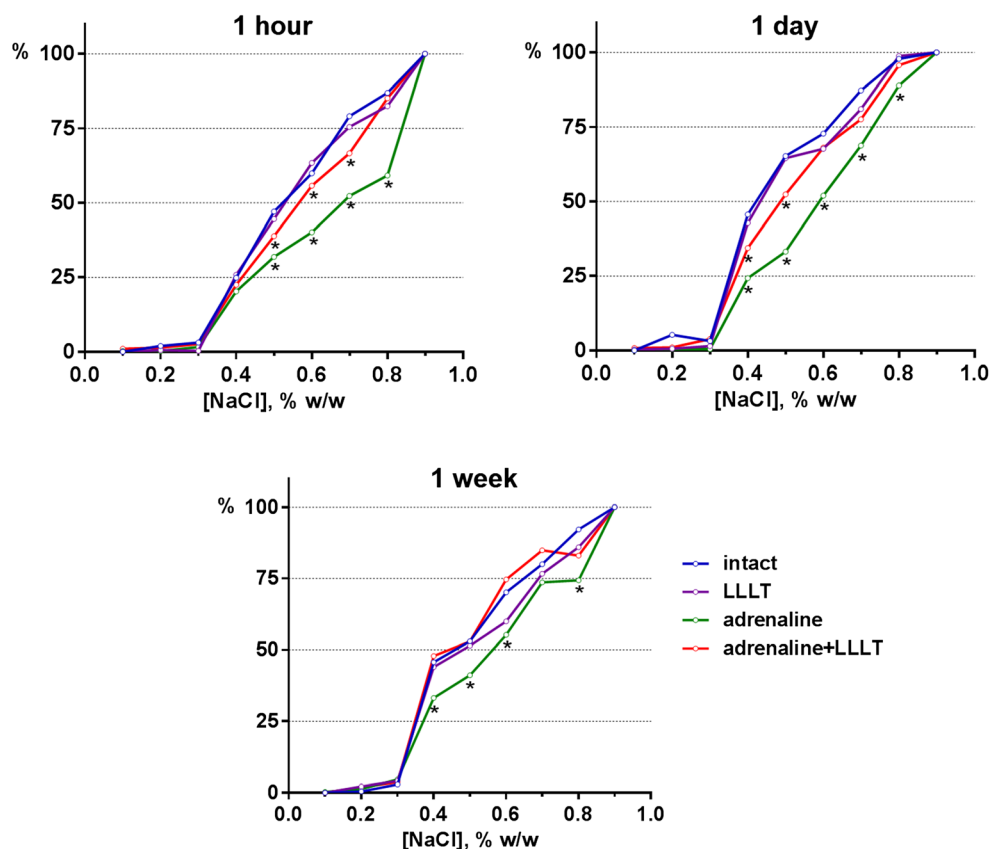
Table 1 The dynamics of the hemoglobin concentration, RBC amount, and electrophoretic mobility in animal groups with various treatments

Parameter	Time after adrenaline administration	Treatment group				
		Intact	LLLT	Adrenaline	Adrenaline+LLLT	Saline
RBC amount ($\times 10^{12}$ cell/l)	1 h	6.8 ± 1.4	$4.2 \pm 0.3^*$	$4.8 \pm 0.2^*$	$4.5 \pm 0.7^*$	6.4 ± 0.9
	1 day	6.5 ± 0.4	6.6 ± 0.9	$4.4 \pm 0.6^*$	$5.4 \pm 0.1^*$	6.6 ± 0.8
	1 week	6.1 ± 0.6	6.2 ± 0.9	$3.9 \pm 0.4^*$	$5.9 \pm 0.7\#$	6.3 ± 0.7
Hemoglobin concentration (g/l)	1 h	113.0 ± 2.4	$77.2 \pm 4.5^*$	$84.0 \pm 3.1^*$	$76.0 \pm 10.8^*$	109.2 ± 1.2
	1 day	106.0 ± 2.8	108.1 ± 5.7	$80.0 \pm 5.0^*$	$93.5 \pm 3.5^*$	111.3 ± 1.3
	1 week	104.2 ± 7.2	95.5 ± 3.3	$86.0 \pm 4.8^*$	$97.8 \pm 5.3\#$	108.4 ± 1.9
EEM ($\mu\text{m} \times \text{cm} / \text{V} / \text{s}$)	1 h	1.23 ± 0.06	$1.59 \pm 0.08^*\#$	$1.12 \pm 0.04^*$	1.15 ± 0.08	1.15 ± 0.05
	1 day	1.32 ± 0.06	$1.46 \pm 0.07\#$	$1.10 \pm 0.06^*$	$1.41 \pm 0.02\#$	1.26 ± 0.04
	1 week	1.22 ± 0.07	$1.54 \pm 0.05^*\#$	$1.07 \pm 0.05^*$	$1.36 \pm 0.09\#$	1.24 ± 0.03

*Statistically significant difference from “intact” group, $p < 0.05$

#Statistically significant difference from “adrenaline” group, $p < 0.05$

Fig. 7 The dynamics of the RBCs osmotic fragility in the animal groups at 1 h, 1 day, and 1 week after treatment. The percentage of RBC resistance to hemolysis is presented. Asterisk indicates values that differ from the value in the intact animals group at $p < 0.05$



channels, which increases the outflux of potassium caused by Na,K-ATPase inhibition and leads to a cell volume compression [26, 27]; (iv) the increase in intracellular Ca^{2+} in RBCs leads to an activation of a scramblase, which causes an exposure of phosphatidylserine to the external surface of RBCs [28, 29]; and (v) the phosphatidylserine exposure to the RBCs external surface induces changes in a cell shape with the formation of echinocytes and stomatocytes [30].

To summarize the results, the registered alterations in the RBCs morphofunctional characteristics under the action of adrenaline are typical for stress. The oxidative processes resulted in a decreased cell charge and an elevated number of the pathologically changed RBCs forms, which is accompanied by a decrease in the osmotic resistance of the cells. A high osmotic fragility is an undesirable effect, since RBCs become more sensitive to changes in blood plasma composition and are easily destroyed. In turn, the reduction of the negative charge of erythrocytes leads to a decreased suspension stability and oxygen transport function of blood [31]. The RBC aggregates can clog the microvasculature and cause blood flow slowdown, which ultimately lead to an adverse changes in the blood macro-rheological parameters [32].

LLLT stimulated the development of adaptation processes, which was expressed in a growth of the RBC membrane electronegativity and recovering of the RBCs osmotic resistance. The normalization of the RBCs osmotic fragility was

accompanied by an increase in the RBC amount in peripheral blood. The elevated electronegativity of the RBCs membranes is of high importance, since it leads to improving the rheological properties of blood and microcirculation. It has been reported that LLLT increases oxygen delivery to tissues [33].

It can be assumed that the LLLT action in the experiment conditions can be realized directly through the influence on blood cells flowing through the irradiated area of the head, and through an adaptive effect of the laser irradiation on the neuroendocrine structures of the brain. The direct LLLT action is mediated by chromophores such as hemoglobin, myoglobin, cytochrome oxidase, other cytochromes, flavin, flavoproteins, and porphyrins [34], as well as by changes in the cell redox potential through an increased ROS generation [35, 36]. As a result, the protein-lipid membrane structure of RBCs changes [37]. Lipid composition and bilayer asymmetry have been shown to affect the overall RBCs shape, as well as the deformability of the cells.

Changes in cytoskeletal proteins that connect the bilayer and spectrin network affect the integrity of the RBC membrane under tangential stresses [38]. Probably, LLLT can induce the recovery of the stress-induced alterations of the RBC protein-lipid membrane, which is manifested in the restoring shape, membrane surface electronegativity, and osmotic stability of RBCs. It is important to note that the optical density of the RBC phase portraits is also restored under LLLT in addition

to the recovering processes of the RBC membrane architectonics. This observation indicates a decrease in the oxidative processes caused by adrenaline, and the restoration of the hemoglobin structure [39]. At the same time, we have recently reported that EEM can serve as an indicator of a stress-reaction and its elevation indicates the development of adaptation processes in the body through the activation of the pituitary-adrenal system [40]. The registered increase in EEM under the LLLT action may reflect the development of general regularities of the homeostasis of the body associated with the restriction of the stress response and activation of the pituitary-adrenal system.

Thus, LLLT causes the mitigation of the stress response and can accelerate the development of adaptation processes. The obtained results can be used for the development of the protocols of LLLT application for correction of microcirculation of organs and tissues under inflammation accompanied with ischemic processes.

Funding The work was financially supported by the Ministry of Science and Higher Education of the Russian Federation (contract no. 14.Z50.31.0022).

Compliance with ethical standards

The animals were housed and the experiment was performed in accordance with Universal Declaration of animal rights and with the Order of the Ministry of Health of the Russian Federation No. 199n of April 1, 2016, “Approval of the good laboratory practice.” All procedures performed in studies involving animals were in accordance with the ethical standards of Lobachevsky University.

Ethical approval All applicable international, national, and institutional guidelines for the care and use of animals were followed. All procedures performed in studies involving animals were in accordance with the ethical standards of Lobachevsky University.

Conflict of interest The authors declare that they have no conflict of interest.

Publisher's note Springer Nature remains neutral with regard to jurisdictional claims in published maps and institutional affiliations.

References

1. Micheli L, Di Cesare Mannelli L, Lucarini E, Cialdai F, Vignali L, Ghelardini C, Monici M (2017) Photobiomodulation therapy by NIR laser in persistent pain: an analytical study in the rat. *Lasers Med Sci*. 32(8):1835–1846. <https://doi.org/10.1007/s10103-017-2284-9>
2. Ray M (2017) Laser therapy and osteoarthritis disability: an update of an unresolved topic. *Nov Tech Arthritis Bone Res* 2(2):555585. <https://doi.org/10.19080/NTAB.2017.02.555585>
3. Lio G-Y, Sun L, Liu TC-Y (2012) Aquaporin-1-mediated effects of low level He-Ne laser irradiation on human erythrocytes. *Int J Photoenergy* 2012:275209–275214. <https://doi.org/10.1155/2012/275209>
4. Joukar A, Nammakie E, Niroomand-Oscuii H (2015) A comparative study of thermal effects of 3 types of laser in eye: 3D simulation with bioheat equation. *J Therm Biol* 49–50:74–81. <https://doi.org/10.1016/j.jtherbio.2015.02.004>
5. Huang YY, Chen AC, Carroll JD, Hamblin MR (2011) Biphasic dose response in low level light therapy—an update. Formerly *Nonlinear Biol Toxicol Med* 9:602–618. <https://doi.org/10.2203/dose-response.11-009>
6. Karu TI, Pyatibrat LV, Kolyakov SF, Afanasyeva NI (2009) Absorption measurements of cell monolayers relevant to mechanisms of laser phototherapy: reduction or oxidation of cytochrome c oxidase under laser radiation at 632.8 nm. *Photomed Laser Surg* 26(6):593–599. <https://doi.org/10.1089/pho.2008.2246>
7. Barolet D, Duplay P, Jacomy H, Auclair M (2010) Importance of pulsing illumination parameters in low-level-light therapy. *J Biomed Opt* 15(4):048005–048007. <https://doi.org/10.1117/1.3477186>
8. Wu S, Xing D, Gao X, Chen WR (2009) High fluence lowpower laser irradiation induces mitochondrial permeability transition mediated by reactive oxygen species. *J Cell Physiol* 218:603–611. <https://doi.org/10.1002/jcp.21636>
9. Moriyama Y, Nguyen J, Akens M (2009) In vivo effects of low level laser therapy on inducible nitric oxide synthase. *Lasers Surg Med* 41(3):227–231. <https://doi.org/10.1002/lsm.20745>
10. Zhang L, Xing D, Zhu D, Chen Q (2008) Low-power laser irradiation inhibiting Abeta25-35-induced PC12 cell apoptosis via PKC activation. *Cell Physiol Biochem* 22(1–4):215–222. <https://doi.org/10.1159/000149799>
11. Liu H, Colavitti R, Rovira II, Finkel T (2005) Redox-dependent transcriptional regulation. *Circ Res* 97:967–974. <https://doi.org/10.1161/01.RES.0000188210.72062.10>
12. Rizzi CF, Mauriz JL, Freitas Corra DS et al (2006) Effects of low-level laser therapy (LLLT) on the nuclear factor (NF)-kappaB signaling pathway in traumatized muscle. *Lasers Surg Med* 38:704–713. <https://doi.org/10.1002/lsm.20371>
13. Aimbire F, Santos FV, Albertini R (2008) Low-level laser therapy decreases levels of lung neutrophils anti-apoptotic factors by a NF-kappaB dependent mechanism. *Int Immunopharmacol* 8(4):603–605. <https://doi.org/10.1016/j.intimp.2007.12.007>
14. Saygun I, Karacay S, Serdar M (2008) Effects of laser irradiation on the release of basic fibroblast growth factor (bFGF), insulin like growth factor-1 (IGF-1), and receptor of IGF-1 (IGFBP3) from gingival fibroblasts. *Lasers Med Sci* 23(2):211–215. <https://doi.org/10.1007/s10103-007-0477-3>
15. Kushibiki T, Hirasawa T, Okawa S, Ishihara M (2015) Low reactive level laser therapy for mesenchymal stromal cells therapies. *Stem Cells Int* 2015:974864, 12 page. <https://doi.org/10.1155/2015/974864>
16. Floras J (2009) Sympathetic nervous system activation in human heart failure: clinical implications of an updated model. *J Am Coll Cardiol* 54(5):375–385. <https://doi.org/10.1371/journal.pone.0094234>
17. Grassi G, Bolla G, Quarti-Trevano F, Arenare F, Brambilla G, Mancia G (2008) Sympathetic activation in congestive heart failure: reproducibility of neuroadrenergic markers. *Eur J Heart Fail* 10(12):1186–1191. <https://doi.org/10.1016/j.ejheart.2008.09.013>
18. Tashireva LA, Perelmuter VM, Denisov EV, Savelieva OE, Kaygorodova EV, Zavyalova MV, Mansikh VN (2017) Types of immune-inflammatory responses as a reflection of cell–cell interactions under conditions of tissue regeneration and tumor growth. *Biochem (Moscow)* 82(5):542–555. <https://doi.org/10.1134/S0006297917050029>
19. Chertok VM, Kotsyuba AE, Bepalova EV (2008) Role of nitric oxide in the reaction of arterial vessels to laser irradiation. *Bull Exp Biol Med* 145(6):751–754. <https://doi.org/10.1007/s10517-008-0186-3>

20. Hilário S, Saldanha C (2003) Martins e Silva J. An in vitro study of adrenaline effect on human erythrocyte properties in both gender. *Clin Hemorheol Microcirc* 28:89–98
21. Brazhe NA, Brazhe AR, Pavlov AN, Erokhova LA, Yusipovich AI, Maksimov GV, Mosekilde E, Sosnovtseva OV (2006) Unraveling cell processes: interference imaging interwoven with data analysis. *J Biol Phys* 32:191. <https://doi.org/10.1007/s10867-006-9012-1>
22. Boyarinov GA, Yakovleva EI, Zaitsev RR, Bugrova ML, Boyarinova LV, Solov'eva OD, Deryugina AV, Shumilova AV, Filippenko ES (2017) Pharmacological correction of microcirculation in rats suffering from traumatic brain injury. *Cell Tissue Biol* 11(1):65–72. <https://doi.org/10.1134/S1990519X17010023>
23. Moroz VV, Molchanova LV, Gerasimov LV, Ostapchenko DA, Yershova LI, Likhovetskaya ZM, Gorbunova NA (2006) Blood rheological and hemolytic effects of perfluorane in patients with severe injury and blood loss. *Gen Reanimatol* 2(1):5–11. <https://doi.org/10.15360/1813-9779-2006-1-5-11>
24. Kushibiki T, Hirasawa T, Okawa S, Ishihara M (2013) Blue laser irradiation generates intracellular reactive oxygen species in various types of cells. *Photomed Laser Surg* 31(3):95–104. <https://doi.org/10.1089/pho.2012.3361>
25. Forman HJ, Fukuto JM, Tottes M (2004) Redox signaling: thiol chemistry defines which reactive oxygen and nitrogen species can act as second messengers. *Am J Physiol Cell Physiol* 287(2):246–256. <https://doi.org/10.1152/ajpcell.00516.2003>
26. Xie Z (2003) Molecular mechanism of Na/K-ATPase-mediated signal transduction. *Ann N Y Acad Sci USA* 986:497–503. <https://doi.org/10.1124/mi.3.3.157>
27. Kucherenko YV, Wagner-Britz L, Bernhardt I, Lang F (2013) Effect of chloride channel inhibitors on cytosolic Ca²⁺ levels and Ca²⁺-activated K⁺ (Gardos) channel activity in c human red blood cells. *J Membrane Biol* 246(4):315–326. <https://doi.org/10.1007/s00232-013-9532-0>
28. Andrews DA, Yang L, Low PS (2002) Phorbol ester stimulates s protein kinase C-mediated agtoxin-TK-sensitive calcium permeability pathway human red blood cell. *Blood* 100:3382–3392. <https://doi.org/10.1182/blood.V100.9.3392>
29. Maellaro E, Leoncini S, Moretti D et al (2013) Del Bello B., Tanganelli I., De Felice C., Ciccoli L. Erythrocyte caspase-3 activation and oxidative imbalance in erythrocytes and in plasma of type 2 diabetic patients. *Acta Diabetol* 50:489. <https://doi.org/10.1007/s00592-011-0274-0>
30. Koshkaryev A, Yedgar S, Relevy H (2003) Acridine orange induced translocation of phosphatidylserine of red blood cell surface. *Am J Physiol Cell Physiol* 285:720–722. <https://doi.org/10.1152/ajpcell.00542.2002>
31. Deryugina AV, Shumilova AV, Filippenko ES, Galkina YV, Simutis IS, Boyarinov GA (2017) Functional and biochemical parameters of erythrocytes during mexicor treatment in posttraumatic period after experimental blood loss and combined traumatic brain injury. *Bull Exp Biol Med* 164(1):26–29. <https://doi.org/10.1007/s10517-017-3918-4>
32. Sprague R, Ellsworth M, Stephenson A, Klein-henz M (2010) Deformation-induced ATP release from red blood cells requires CFTR activity. *Am Physiol Soc* 275:H1726–P1732
33. Yesman SS, Mamilov SO, Veligotsky DV, Gisbrecht AI (2016) Local changes in arterial oxygen saturation induced by visible and near-infrared light radiation. *Lasers Med Sci* 31(1):145–149. <https://doi.org/10.1007/s10103-015-1838-y>
34. Hamblin MR, Demidova-Rice TN (2007) Cellular chromophores and signaling in LLLT. In: Hamblin MR et al (eds) *Mechanisms for low-light therapy II. The International Society for Optical Engineering*, Bellingham. <https://doi.org/10.1201/9781315364827>
35. Chen AC, Arany PR, Huang YY, Tomkinson EM, Sharma SK et al (2011) Low level laser therapy activates NF-κB via generation of reactive oxygen species in mouse embryonic fibroblasts. *PLOS One*. 6(7):e22453. <https://doi.org/10.1371/journal.pone.0022453>
36. Zhang J, Xing D, Gao X (2008) Low-power laser irradiation activates Src tyrosine through reactive oxygen species-mediated signaling pathway. *J Cell Physiol* 217(2):518–528. <https://doi.org/10.1002/jcp.21697>
37. Kujawa J, Pasternak-Mnich K, Zawodnik IB, Irzmański R (2014) The effect of near-infrared MLS laser radiation on cell membrane structure and radical generation. *Lasers Med Sci* 29(5):217. <https://doi.org/10.1007/s10103-014-1571-y>
38. Bennett-Guerrero E, Veldman TH, Doctor A, Telen MJ, Ortel TL, Reid TS, Mulherin MA, Zhu H, Buck RD, Califf RM (2007) Evolution of adverse changes in stored RBCs. *Proc Natl Acad Sci USA* 104(43):17063–17,068. <https://doi.org/10.1073/pnas.0708160104>
39. Deryugina AV, Ivashchenko MN, Ignatiev PS, Talamanova MN, Samodelkin AG (2018) The capabilities of interference microscopy in studying the in vitro state of erythrocytes exposed to low-intensity laser radiation for stress correction. *Sovremennyye Tehnol Med* 10(4):78–83. <https://doi.org/10.17691/stm2018.10.4.09>
40. Deryugina AV, Ivashchenko MN, Ignatyev PS, Zolotova MV, Samodelkin AG (2018) The electrophoretic mobility of erythrocytes and micronucleus test of buccal cells as a stress intensity marker. *Int J Biomed* 8(4):347–350. [https://doi.org/10.21103/Article8\(4\)_OA16](https://doi.org/10.21103/Article8(4)_OA16)